Available online at www.sciencedirect.com
ScienceDirect
Procedia Engineering 2 (2010) 1839–1847
Procedia Engineering
www.elsevier.com/locate/procedia

Fatigue 2010

Investigation of variability in fatigue crack nucleation and propagation in alpha+beta Ti-6Al-4V

Patrick J. Golden[a*], Reji John[a], W. John Porter, III[b]

[a]US Air Force Research Laboratory, AFRL/RXLMN, Wright-Patterson AFB, OH 45433, USA
[b]University of Dayton Research Institute, Dayton, OH 45469, USA

Received 8 March 2010; revised 10 March 2010; accepted 15 March 2010

Abstract

The understanding of fatigue variability in turbine engine materials is vital to permit a reduction of US Air Force sustainment costs through fatigue life extension and/or inspection interval extension. Additionally, the US Air Force is currently moving further towards the use of probabilistic damage tolerance design methods. These probabilistic models require not only a good understanding of the variability in specimen data, but also an understanding of the microstructural sources of variability to allow scaling to component analysis.

The objective of this work was to study the fatigue variability of a common turbine engine alloy Ti-6Al-4V. Typical testing consisted of smooth bar fatigue tests at multiple stress ratios and stress levels in order to generate a fully populated stress-life curve. These tests, however, typically do not consist of many repeats. The approach of this work was to conduct a statistically significant number of repeated fatigue tests at several loading conditions. A similar approach has been performed on several other turbine engine material systems often revealing bimodal life distributions consisting of a number of low life specimens that may fail due to a separate mechanism. This paper discusses the Ti-6Al-4V life distributions and sources of variability. Crack propagation using small crack growth data was used to predict the lower tail of the life distributions.

Keywords: Fatigue Nucleation; Fatigue Crack Growth; Life Variability; Ti-6Al-4V; Small Crack Growth; Surface Condition

1. Introduction

The current life management approach for maintaining fracture critical turbine engine components in the US Air Force is based on the specification known as the Engine Structural Integrity Program [1]. This specification is based on traditional views of statistical behavior of materials and is often very conservative resulting in high sustainment costs. The Air Force is, therefore, pursuing physics or mechanics-based probabilistic material behavior models to handle the understanding and modeling of the sources of uncertainty in fatigue behavior under service conditions. These models are based on observed damage mechanisms and, therefore, predictions of design fatigue limits can be expected to be more accurate than data based statistical estimations. Examples of physics-based probabilistic fatigue life prediction models include the approaches proposed by Magnusen et al. [2], Chan et al. [3], Tryon et al. [4], Laz et al. [5], and Jha et al. [6-7]. Jha has shown that materials often exhibit a dual failure mode that is stress dependent that is often only observable when fatigue testing is conducted with large sample sizes. The objective of

* Corresponding author. Tel.: +1-937-255-5438; fax: +1-937-656-4840.
E-mail address: patrick.golden@wpafb.af.mil.

1877-7058 © 2010 Published by Elsevier Ltd.
doi:10.1016/j.proeng.2010.03.198

Report Documentation Page

Form Approved
OMB No. 0704-0188

1. REPORT DATE	2. REPORT TYPE	3. DATES COVERED
10 MAR 2010		**00-00-2010 to 00-00-2010**

4. TITLE AND SUBTITLE	5a. CONTRACT NUMBER
Investigation of variability in fatigue crack nucleation and propagation in alpha+beta Ti-6Al-4V	5b. GRANT NUMBER
	5c. PROGRAM ELEMENT NUMBER
6. AUTHOR(S)	5d. PROJECT NUMBER
	5e. TASK NUMBER
	5f. WORK UNIT NUMBER
7. PERFORMING ORGANIZATION NAME(S) AND ADDRESS(ES) **Air Force Research Laboratory,AFRL/RXLMN,Wright-Patterson AFB,OH,45433**	8. PERFORMING ORGANIZATION REPORT NUMBER
9. SPONSORING/MONITORING AGENCY NAME(S) AND ADDRESS(ES)	10. SPONSOR/MONITOR'S ACRONYM(S)
	11. SPONSOR/MONITOR'S REPORT NUMBER(S)

12. DISTRIBUTION/AVAILABILITY STATEMENT
Approved for public release; distribution unlimited

13. SUPPLEMENTARY NOTES

14. ABSTRACT
see report

15. SUBJECT TERMS

16. SECURITY CLASSIFICATION OF:			17. LIMITATION OF ABSTRACT	18. NUMBER OF PAGES	19a. NAME OF RESPONSIBLE PERSON
a. REPORT **unclassified**	b. ABSTRACT **unclassified**	c. THIS PAGE **unclassified**	**Same as Report (SAR)**	**9**	

this research is to experimentally investigate the variability in total fatigue life, crack nucleation and growth of an alpha+beta processed Ti-6Al-4V alloy [8]. This work builds on the previously reported study in Golden et al. [9]. The applied stress conditions in which a dual mode fatigue behavior is observed is of particular interest. The effect of surface finish and surface residual stress are also observed in the data and discussed. Modeling of the crack growth life and the relation to the fatigue life distribution was also investigated.

2. Experimental Methods

The material used for this study was an alpha+beta forged Ti-6Al-4V alloy 8]. The material was forged to plates approximately 40 cm by 15 cm by 2 cm in dimension. Post forging, the material was solution treated and overaged at 932°C for 75 min, fan cooled, and mill annealed at 704°C for 2 hr. The resulting microstructure was approximately 60% primary alpha and 40% transformed beta. The elastic modulus was 116 GPa and the 0.2% offset yield stress was 930 MPa. The ultimate tensile strength was 980 MPa. The round bar fatigue specimens, shown in Fig. 1, were machined from the forged plate in the long direction of the plate. The gauge section diameter is 4.27 mm and the gauge length is 12.7 mm. The gauge section of all specimens was finished using longitudinal low stress grinding (LSG) followed by polish. This surface finish process will be referred to simply as LSG throughout this paper. In many of the specimens, this finishing step was followed by additional time at the mill annealing temperature of 704°C for 1 hr, followed by electro-polishing to remove approximately 25 μm of material. The purpose of this process is to remove surface layer residual stresses induced by machining, and this surface finish will be referred to simply as electro-polish (EP) throughout this paper. The surface roughness of the LSG specimens was approximately 0.2 μm, while it was approximately 0.05 μm on the EP specimens.

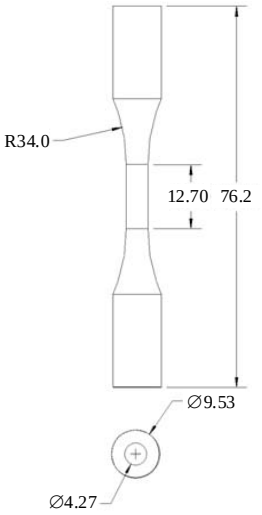

Figure 1: Drawing of the test specimen used in this project (dimensions in mm).

Fatigue testing was performed at constant amplitude loading with a stress ratio, *R*, of 0.1. A limited number of different maximum stresses were chosen that would result in lives on the order of 10,000 to 10^7 cycles. The objective of the research was to study variability at different surface conditions, so only a few maximum stress values were chosen to permit a significant number of repeat tests at each condition. Four maximum stress values were chosen for this study; 600 MPa, 635 MPa, 675 MPa, and 750 MPa, that were tested at both surface conditions. These stresses were expected to produce behavior in the typical test specimen that ranged from relatively short nucleation life and dominated by propagation life, to very long nucleation life. However, the objective of this work was to investigate not just the typical behavior, but the variability in behavior to eventually lead to better

understanding of the mechanisms that drive the variability. To that end, the number of specimens tested at each surface condition and stress level ranged from a minimum of 10 at 750 MPa to 22 at 675 MPa. In total, 132 specimens that have been tested are reported here. Finally, some of the specimens were periodically stopped for surface replication. Acetate tape replicas were taken at fixed increments of loading, typically 5000-7500 cycles for 675 MPa and 635 MPa maximum stresses respectively. At the end of the test, the primary crack was tracked back to its earliest possible observation resulting in surface crack length, 2a, versus cycles, N, data.

3. Analytical Methods

To support the analysis of the fatigue test results, fracture mechanics crack growth predictions have been made including predictions for cracks approaching those that are small relative to the microstructure. The typical primary alpha grain size in this material is approximately 15 μm, and a 30 x 15 μm semi-elliptical surface crack was chosen as the initial crack size in a deterministic crack growth analysis. This assumption is discussed further in the next section. Here, 15 μm is the crack depth, a, and 30 μm is the full surface length, $2c$. The mode I stress-intensity factor, K_I, solution used for the tensile applied loading was the surface crack in a round bar solution by Raju and Newman [10]. In the case of the LSG surface condition, however, a surface residual stress gradient was present that had potential to affect the short crack propagation life of the specimens. The total stress intensity factor, K_{tot}, was therefore calculated according to Equation 1.

$$K_{tot} = K_{app} + K_{res} \tag{1}$$

Here K_{app} is calculated using the round bar solution, however, K_{res} is calculated using a weight function solution for a surface crack in a rectangular plate [11]. A rectangular plate weight function solution was chosen since no weight function solution was available for a surface crack in a round bar. It was reasoned that the rectangular plate solution would be sufficient in this case since the LSG residual stress distribution was expected to be very shallow and would therefore only affect K for cracks very small relative to the geometry. To validate this assumption, a three-dimensional finite element model was developed for both the round bar and square plate geometries using the same boundary conditions assumed in the K solutions. The dimensions of the square plate were chosen to equal the diameter of the rod. The fracture mechanics software, FRANC3D/NG [12], was used to insert several size cracks and to calculate the resulting mode I stress intensity factors due to the applied load and the LSG residual stress distribution. Fig. 2 has plots of K_{res} at the surface, c, and maximum depth, a, as a function of crack size from FRANC3D/NG for the round bar and a square plate, and also the rectangular plate weight function solution. It appears that there were significant differences between the weight function solution for the square plate and the FRANC3D/NG results, however, the assumption that K_{res} for the round bar could be replaced by K_{res} for the square plate appeared to be reasonable.

The fracture mechanics crack growth life predictions were then performed using the K solution as described above. The crack growth rate model used was a Paris Law fit to a combination of short crack and long crack growth da/dN versus ΔK data at R = 0.1 collected from several efforts for this Ti-6Al-4V material and further described in Golden, et al [9] and described in equation 2.

$$da/dN = 3.45x10^{-11}\Delta K^{3.02} \tag{2}$$

The Paris Law fit was a reasonable approximation for handling the combined short crack and long crack data since the short cracks were found to have an accelerated crack growth rate and the average behavior tended to follow a straight power law fit with no threshold value. Equation 2 was integrated to find crack propagation life using the Euler method starting from the assumed initial crack size of 15 μm with a/c = 1.

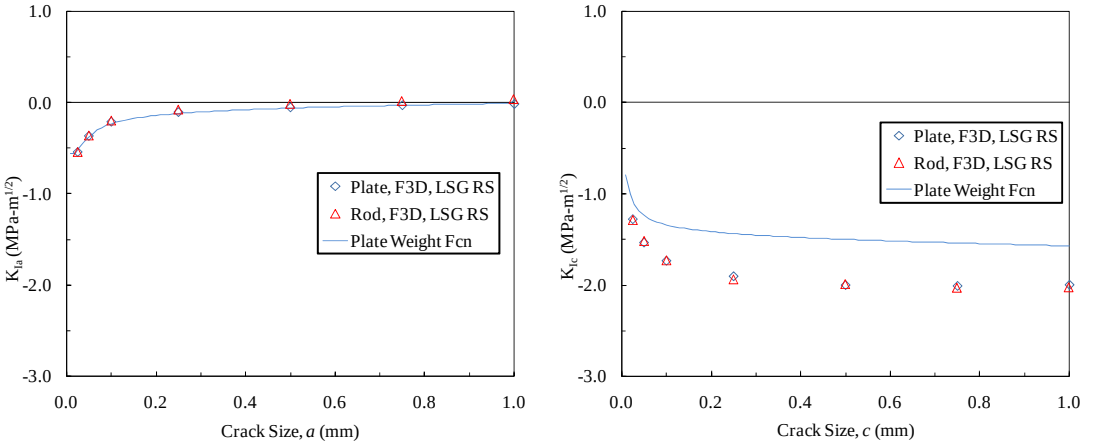

Figure 2: Comparison of FRANC3D/NG (F3D) and weight function K solutions.

4. Results and Discussion

The complete set of fatigue test results is plotted in Fig. 3. The circles are the EP specimens, and the triangles are the LSG specimens. All tests were conducted at $R = 0.1$ at maximum stresses of 600, 635, 675, and 750 MPa. The LSG and EP plotted points were offset plus or minus 5 MPa, respectively, from the actual applied stress for clarity on the plot. The solid lines are the geometric mean values for each surface condition. A few observations can be made from these results. First, it was interesting that the difference in mean life between EP and LSG was quite dependent on stress. At high stress, the mean failure life was significantly shorter in the EP specimens, however, at low stress this trend begins to reverse. In fact, if one looked at the median rather than mean failure life, it is longer in the EP specimens at 600 MPa than for the LSG specimens. The scatter or variability in life followed a very different trend. The LSG specimens have approximately the same scatter at all applied stress levels, however, the scatter in the EP results was highly dependent on the stress level. The scatter at 750 MPa was very small and increased to 3 orders of magnitude at 600 MPa. Much like what had been observed in other materials [6,7,13], the behavior of the EP specimens seemed to have a stress dependent bimodal behavior, where failures can be split into two groups, called simply “short lives” and “long lives.” As the applied stress increased the likelihood of short lives appears to increase, while as the stress decreases the number of long lives appears to increase. The LSG specimens do not seem to follow this trend. There were no clear groupings defining short and long lives and the variability had much less dependence on stress.

There were two competing mechanisms that helped explain the differences in variability and mean behavior of the EP and LSG specimens. First, the surface residual stresses were significantly different by design, and secondly, the surface finishes were different. LSG is a machining process designed to impart a well controlled compressive residual stress on the surface of the material. It was followed by a mechanical polish in the longitudinal direction. Conversely, EP was intentionally chosen to remove those residual stresses imparted by LSG as well as leave a highly polished surface finish. The surface roughness, R_a, of EP and LSG were approximately 0.2 μm and 0.05 μm, respectively. Fig. 4 shows the measured transverse residual stresses in the EP and LSG specimens. The residual stresses were measured using x-ray diffraction with electropolishing for layer removal. The stresses plotted were corrected for stress gradient and layer removal. The LSG samples had surface values ranging from -250 to -300 MPa decreasing to near zero within approximately 25 μm. The EP samples had approximately 25 MPa residual stress on the surface, and were very similar to LSG in the subsurface. It was expected that this difference in surface residual stress state could impact both the crack nucleation behavior and the short crack growth behavior.

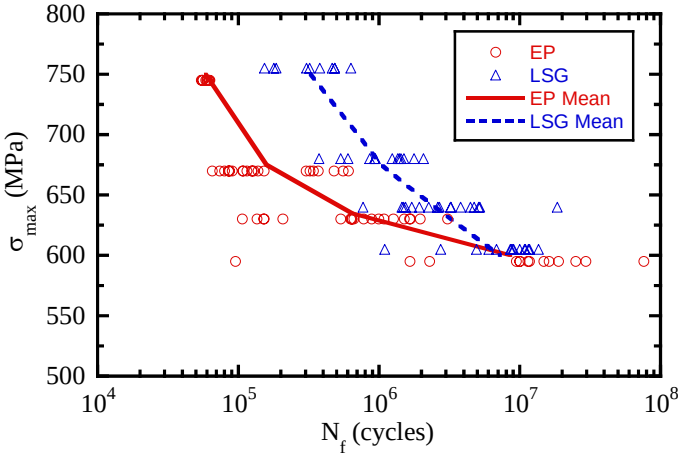

Figure 3: Fatigue test data at R = 0.1 with solid lines on the means of the EP and LSG data (the data are offset +/- 5MPa for clarity.)

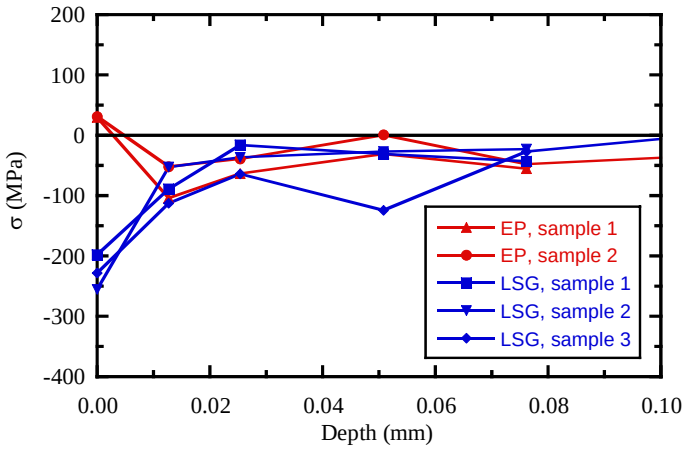

Figure 4: Residual stresses measurements from EP and LSG specimens.

Since it was hypothesized that one of the mechanisms leading to differences in the EP and LSG behavior was the influence of residual stresses on short crack growth, a crack growth analysis was performed as described in the previous section. The LSG residual stress distributions were fit to a curve. The EP residual stress field was simply assumed to be zero. The initial crack size was assumed to equal 15 μm in depth and 30 μm surface length. This size corresponds to the average primary alpha grain size in the material, which is the microstructural feature at which cracks nucleate. This deterministic analysis was repeated at several stresses between the maximum applied stresses of 500 and 800 MPa at R = 0.1. These fracture mechanics (FM) crack growth life predictions were plotted along with test data in Fig. 5. As expected, the EP crack growth lives lined up fairly well with the minimum life of the specimens at all stresses. This showed that the “short life” specimens have nearly zero nucleation life. Even

though the likelihood that a specimen behaves as a “short life” specimen decreases quickly with decreasing stress, the fracture mechanics crack propagation prediction does a good job of prediction the minimum life associated with the “short life” specimens at all stresses. This supports the hypothesis that in the EP surface condition, the minimum life is controlled by crack growth with very little nucleation life.

The LSG fracture mechanics crack growth predictions do not match the observed minimum experimental lives of the LSG test specimens very well, however. As shown in Fig. 5, the observed minimum specimen fatigue life was between 3 and 8 times greater than the predicted minimum life based on fracture mechanics crack growth. It appears that the longer mean life of the LSG specimens over the EP specimens could not be explained simply by a longer crack growth life. This was not surprising since experimental observations and FM analysis show that the “long life” specimen lives are primarily controlled by nucleation. It, therefore, seems as though the LSG surface finish not only extended the minimum life due to the effect of compressive residual stress on crack growth, but also inhibited the crack nucleation mechanism that led to the “low life” failures. The crystallographic mechanisms that lead to the “low life” failures are the subject of further research.

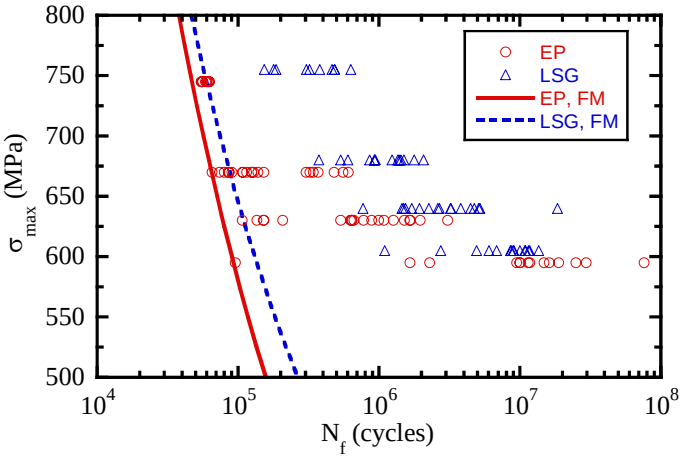

Figure 5: Fatigue test data with the fracture mechanics minimum life predictions (the data are offset +/- 5MPa for clarity.)

Fractography of the LSG and EP specimens was performed to investigate the location and features of the crack nucleation sites. Prior studies on this Ti-6Al-4V [8,9] have shown that in this microstructure cracks start predominantly at or very near the surface from primary alpha grains. In fact, no known specimens nucleated subsurface cracks in tests of this Ti-6Al-4V material as part of the HCF program. Studies of Ti-6Al-2Sn-4Zr-6Mo [6,13] with a very similar microstructure, but higher yield strength, on the contrary, had numerous subsurface cracks nucleate at stresses and lives similar to the Ti-6Al-4V tests in this study. Out of 66 EP specimens and 56 LSG specimens fracture surfaces examined, only 2 nucleated in the subsurface. Example fractographs of surface nucleated cracks are shown in Figs. 6 with a low magnification view of the crack nucleation site with river patterns emanating from the site, and a higher magnification view of the flat facet at the surface from which the crack grows. These flat facets are fractured primary alpha grains. Fig. 7 is one of the two subsurface nucleated cracks. Both subsurface nucleated cracks occurred in EP prepared specimens. None were found in LSG specimens. In the subsurface nucleations, there were many primary alpha grain facets in the center of the crack nucleation region and it was too difficult to determine if any one of these grains was the first to nucleate the primary crack.

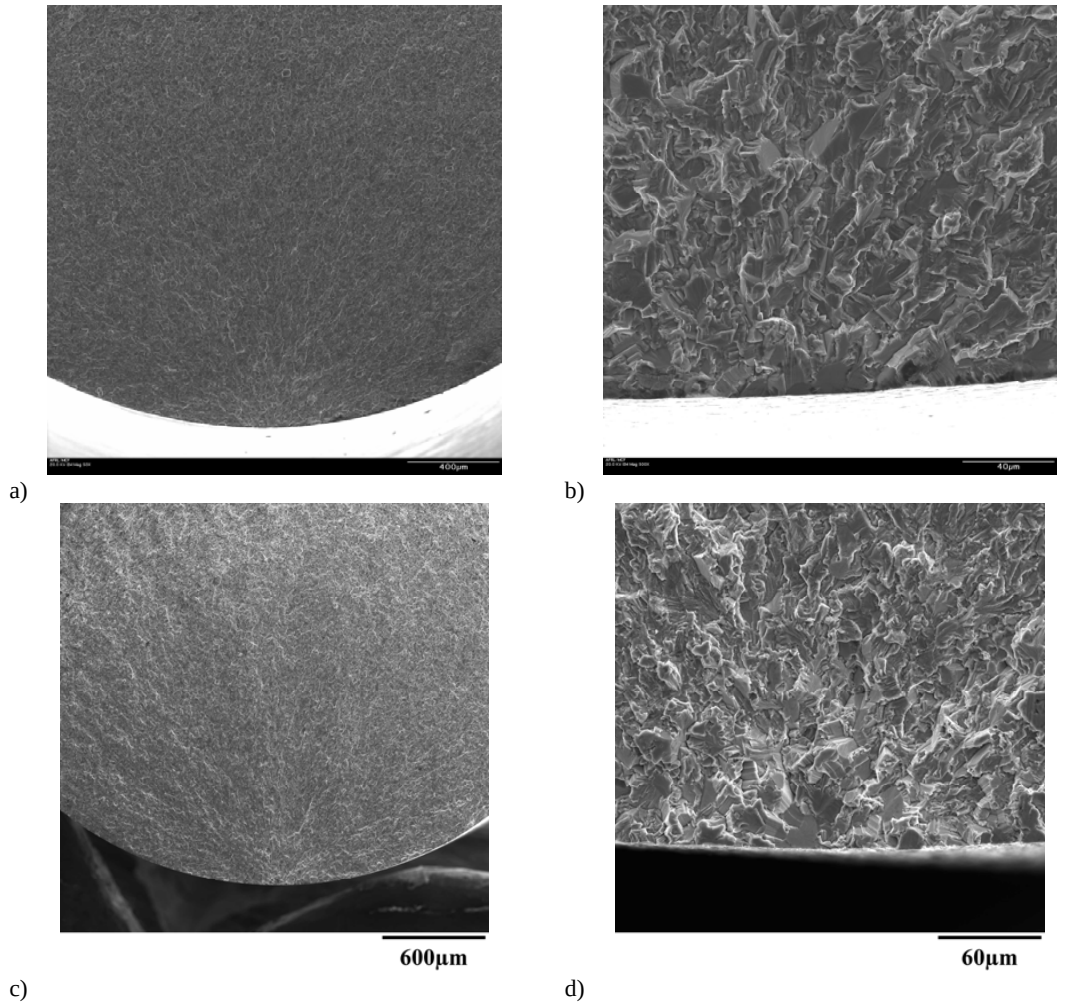

Figure 6: Fractographs of typical surface located primary alpha grain facet initiation site for EP (a and b) and LSG (c and d).

5. Conclusions

Several conclusions were made from this study. Repeated fatigue tests were conducted at 4 stress levels and 2 surface conditions, LSG and EP. Enough tests were conducted at each condition to identify differences in the distributions of the lives to failure at each condition. It was observed that the scatter in the EP specimens increased greatly with decreasing stress, and there appeared to be a dual mode behavior which was also dependent on stress level. This dual mode consisted purely of groups of failures at either “short life” or “long life”, and an initial fractographic study failed to identify a physical mechanism responsible for the differences in life. The scatter in LSG specimen failure lives was much less sensitive to the applied stress. The mean life of the LSG specimens followed a trend of being longer than the EP lives at high stress, but nearly the same at low stress. That observation, combined with the results of a fracture mechanics crack growth prediction lead to the conclusion that the LSG

specimens were dominated by crack nucleation and fall entirely into the “long life” mechanism of failure. It appeared that the LSG surface condition turned off the “short life” crack nucleation mechanism.

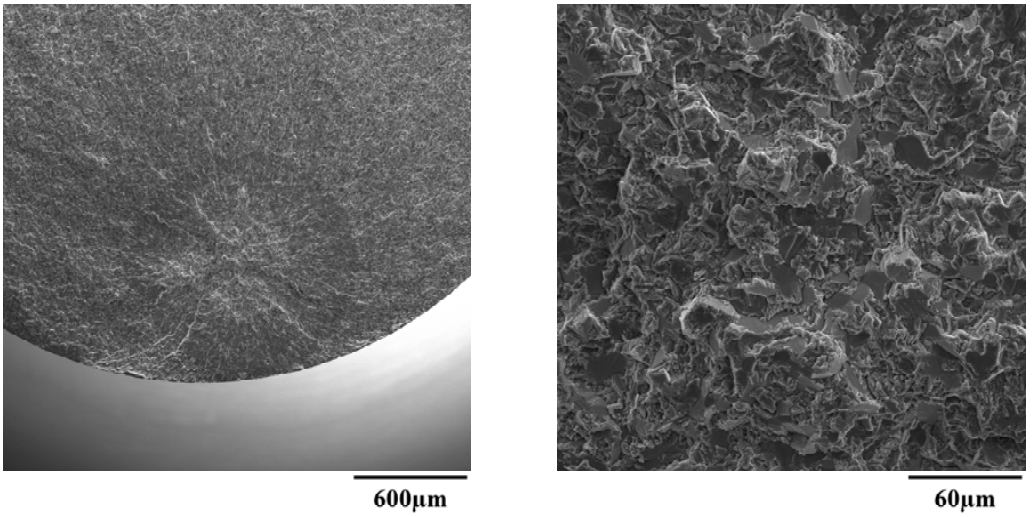

Figure 7: Fractographs (a and b) of a rare internal crack initiation site found in an EP specimen.

Acknowledgements

This work was performed at the Air Force Research Laboratory, AFRL/RXLMN, Materials and Manufacturing Directorate, Wright-Patterson Air Force Base, and was partially supported under AF Contract No. FA8650-09-D-5223 with the University of Dayton Research Institute.

References

[1] U.S. Air Force, Engine Structural Integrity Program, Military Standard 1783B, Aeronautical Systems Center, Wright-Patterson Air Force Base, OH, 31 May 2002.

[2] Magnusen PE, Bucci RJ, Hinkle AJ, Brockenbrough JR, Konish HJ. Analysis and Prediction of Microstructural Effects on Long-Term Fatigue Performance of an Aluminum Aerospace Alloy. *Int J Fat* 1997;**19**:S275–83.

[3] Chan KS, Enright MP. A Probabilistic Micromechanical Code for Predicting Fatigue Life Variability: Model Development and Application. *J Eng Gas Turb Power* 2006;**128**:889-95.

[4] Tryon R. Dey A. Krishnan G. Microstructural-Based Physics of Failure Models to Predict Fatigue Reliability. *J IEST* 2007;**50**:73-84.

[5] Laz PJ. Craig BA. Hillberry BM. A probabilistic Total Fatigue Life Model Incorporating Material Inhomogeneities, Stress Level and Fracture Mechanics. *Int J Fat* 2001;**23**:S119-27.

[6] Jha SK, Larsen JM, Rosenberger AH, Hartman GA. Dual Fatigue Failure Modes in Ti-6Al-2Sn-4Zr-6Mo and Consequences on Life Prediction. *Scripta Mater* 2003;**48**:1637-42.

[7] Jha SK, Caton MJ, Larsen JM. A New Paradigm of Fatigue Variability Behavior and Implications for Life Prediction. *Mat Sci Eng A* 2007;**468-470**:23-32.

[8] “Improved High Cycle Fatigue (HCF) Life Prediction”, Eds. Gallagher, J.P, et al., AFRL-ML-WP-TR-2001-4159, Wright-Patterson AFB, OH 45433.

[9] Golden PJ, John R, Porter WJ, III. Variability in Room Temperature Fatigue Life of Alpha+Beta Processed Ti-6Al-4V. *Int J Fat* 2009;**31**:1764-70.

[10] Raju IS, Newman JC. Stress-Intensity Factors for Circumferential Surface Cracks in Pipes and Rods under Tension and Bending Loads. *Fracture Mechanics: Seventeenth Volume, ASTM STP 905*, JH Underwood, R Chait, CW Smith, DP Wilhem, WA Andrews, JC Newman, Eds., American Society for Testing and Materials, 1986, 789-805.

[11] Murakami Y, Aoki S, Miyata. Stress Intensity Factors Handbook. Pergamon, 1996.

[12] Wawrzynek PA, Carter BJ, Ingraffea AR. Advances in Simulation of Arbitrary 3D Crack Growth using FRANC3D/NG. In: 12th International Conference on Fracture, 2009.

[13] Szczepanski CJ, Jha SK, Larsen JM, Jones JW. Microstructural influences on very high cycle fatigue crack initiation in Ti-6246. *Metall Mater Trans A* 2008;**39A**:2841-51.